Bioorganic & Medicinal Chemistry Letters 26 (2016) 2481–2488

Contents lists available at ScienceDirect

Bioorganic & Medicinal Chemistry Letters

journal homepage: www.elsevier.com/locate/bmcl

Synthesis and characterization of a series of chiral alkoxymethyl morpholine analogs as dopamine receptor 4 (D_4R) antagonists

Jonathan O. Witt [a], Andrea L. McCollum [a], Miguel A. Hurtado [b], Eric D. Huseman [a], Daniel E. Jeffries [a], Kayla J. Temple [a], Hyekyung C. Plumley [b,c], Anna L. Blobaum [b,c], Craig W. Lindsley [a,b,c], Corey R. Hopkins [a,b,c,*]

[a] Department of Chemistry, Vanderbilt University, Nashville, TN 37232, United States
[b] Department of Pharmacology, Vanderbilt University Medical Center, Nashville, TN 37232, United States
[c] Vanderbilt Center for Neuroscience Drug Discovery, Vanderbilt University Medical Center, Nashville, TN 37232, United States

ARTICLE INFO

Article history:
Received 26 February 2016
Revised 25 March 2016
Accepted 28 March 2016
Available online 30 March 2016

Keywords:
Dopamine 4 receptor
Antagonist
Morpholine
L-DOPA-induced dyskinesia
Dopamine Selectivity

ABSTRACT

Herein, we report the synthesis and structure–activity relationship of a series of chiral alkoxymethyl morpholine analogs. Our efforts have culminated in the identification of (*S*)-2-(((6-chloropyridin-2-yl)oxy)methyl)-4-((6-fluoro-1*H*-indol-3-yl)methyl)morpholine as a novel potent and selective dopamine D4 receptor antagonist with selectivity against the other dopamine receptors tested (<10% inhibition at 1 μM against D_1, D_{2L}, D_{2S}, D_3, and D_5).

Dopamine (DA) is a major neurotransmitter and is the primary endogenous ligand for the dopamine receptors. Dopamine receptors are members of the Class A G-protein coupled receptors. There are five dopamine receptor subtypes which are subdivided into two families, the D_1-like family and the D_2-like family. The D_1-like family consists of the D_1 and D_5 receptor subtypes which are coupled to G_s and mediate excitatory neurotransmission. The D_2-family consists of three receptor subtypes (D_2, D_3, and D_4) which are coupled to G_i/G_o and mediate inhibitory neurotransmission. Of the subtypes, the dopamine D_4 receptor (D_4R) has received considerable attention as a potential target for pharmacological intervention due to disorders linked to dysfunction of this receptor (schizophrenia[1–3], Parkinson's disease[4,5], and substance abuse[6–8]).

Recently, we reported on the identification of a chiral morpholine scaffold as a potent and selective D_4R antagonist, ML398 (Fig. 1).[9,10] ML398 was active in vivo; however, the SAR analysis was limited due to the synthetic feasibility of modification of the upper right-hand phenethyl group. Thus, we wanted to evaluate alternative linker groups in order to more fully explore the SAR around both the *N*-linked groups as well as moieties adjacent to the oxygen group of the morpholine.

To this end, we set out to replace the ethyl linker with a hydroxymethyl group as this would allow for significant diversification of this portion of the molecule.[11] In addition, as we have shown previously, the activity of the chiral morpholine scaffold resides in the (*S*)-enantiomer and the starting Boc-protected (*S*)-2-(hydroxymethyl)morpholine is commercially available. The synthetic procedure to access these compounds is shown in Scheme 1. The *tert*-butyl (*S*)-2-(hydroxymethyl)morpholine-4-carboxylate, **1**, was coupled with the appropriate aryl bromide, **2**, under copper mediated conditions to afford **3**.[12] Alternatively, the aryl ethers could be formed under Mitsunobu conditions[13] (ArOH, PPh_3, DIAD, μW, 180 °C) in good yield. Next, the Boc group was removed under acidic conditions and reductive amination with polymer bound $CNBH_3$ provided the final compounds in modest overall yields.[14]

The first set of analogs that we synthesized and evaluated kept the upper right-hand portion constant as the unsubstituted phenoxy moiety and modified the southern nitrogen substituents. A key component for the design of the molecules was to lower the *c*Log*P* of the compounds since ML398 was rather lipophilic (*c*Log*P* = 5.10), with a design on potency and pharmacokinetic parameters. The 4-chlorobenzyl, **4a**, direct comparator to ML398 (K_i = 36 nM) was equipotent to its predecessor compound (K_i = 42 nM) and the introduction of an ether linker led to a significant improvement (lowering) of the *c*Log*P* (5.10 vs. 3.73).[10]

* Corresponding author. Tel.: +1 615 936 6892; fax: +1 615 778 1414.
E-mail address: corey.r.hopkins@vanderbilt.edu (C.R. Hopkins).

http://dx.doi.org/10.1016/j.bmcl.2016.03.102
0960-894X/

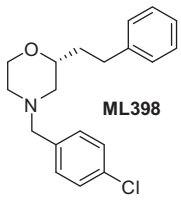

Figure 1. Structure of previously disclosed chiral morpholine D_4 antagonist, ML398.

Further substitution around the benzyl group led to a more active compound (3,4-dimethyl, **4b**, K_i = 12.3 nM). Additional steric bulk was well tolerated as the naphthyl group was active as well (**4d**, K_i = 17.8 nM). Interestingly, the 2-substituted quinoline, **4e**, was significantly less potent (K_i = 310 nM) compared to the naphthyl group. Multiple substitution patterns around the phenyl group are well tolerated (**4f**–**4s**) with a few notable exceptions. Namely, the 3-chloro-4-fluorophenyl (**4f**, K_i = 170 nM) and 3, 4-difluorophenyl (**4h**, K_i = 150 nM) were less potent than the other analogs tested. The transposed 4-chloro-3-fluorophenyl (**4g**, K_i = 19.1 nM) and the 3,4-dichlorophenyl (**4i**, K_i = 27 nM) were more active by ~10-fold, suggesting the 4-fluoro substitution is not as well tolerated. However, this is not a fully general phenomenon as the 3-methoxy-4-fluoro analog, **4m**, is one of the most potent compounds in this series (K_i = 11.6 nM), along with the 3-methoxy-4-chloro compound (**4p**, K_i = 11.6 nM) and 4-methoxy-3-chloro (**4n**, K_i = 10.4 nM). As an additional confirmation of the (*S*)-enantiomer activity, the (*R*)-enantiomer of **4n** was made and evaluated, and it was not active (**4o**, 35% inhibition at 10 μM). In addition to substituted benzyl groups in the southern portion of the molecule, heteroaryl moieties were also well tolerated. The imidazo[1,5-*a*]pyridine, **4u** (K_i = 35 nM), was equipotent with ML398; however, the imidazo[1,2-*a*]pyridine, **4t** (K_i = 160 nM) was less potent. Moving to the 3-substituted indole compounds yielded the most active compounds in this set of analogs. The 6-chloro (**4aa**, K_i = 2.2 nM), 6-methoxy (**4dd**, K_i = 5.4 nM) and 6-fluoro (**4ee**, K_i = 5.2 nM) were all productive changes. The corresponding 5-substituted indole compounds were not as active (**4bb** and **4cc**), nor was a 4-substituted analog (**4ff**).

Next, we turned our attention to the alkoxy substituents (R^2, Table 2) in conjunction with the southern fragments (R^1, Table 1). Initial evaluation utilized the 4-chlorobenzyl and 4-methoxybenzyl groups as these were shown to be potent antagonists of the D_4R.

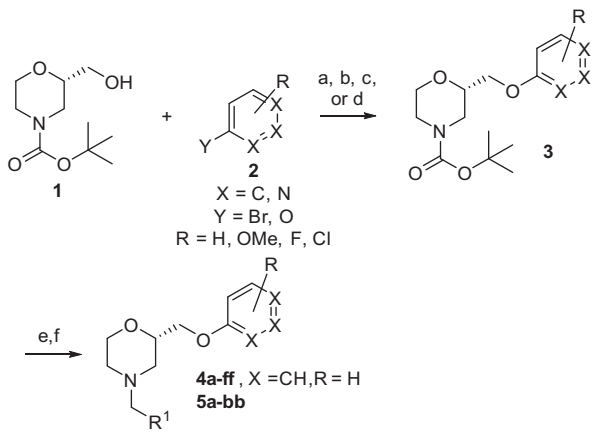

Scheme 1. Reagents and conditions: (a) CuI, Me_4Phen, Cs_2CO_3, toluene (14–30%); (b) ArOH, PPh_3, DIAD, benzene, rt (51%); (c) ArOH, PS-PPh_3, DIAD, THF, rt (21–25%); (d) ArOH, PPh_3, DIAD, THF, μW, 180 °C, 5 min (62%); (e) 4 M HCl in dioxanes; (f) polymer bound $CNBH_3$, R^1CHO, acetic acid, DCM (16–42%).

The first analogs tested were 5-pyrimidine and 2-pyrimidine replacements for the phenyl group. Neither of these replacements led to active compounds; although **5a** did show weak activity (76% inhibition at 10 μM), and introduction of these polar groups led to a significant lowering of the *c*Log*P*, as expected. However, removal of one of the nitrogen atoms in the 5-pyrimidine analog led to the 3-pyridine analog and resulted in significant recovery of the potency (**5e**, K_i = 47 nM; **5f**, K_i = 59 nM). Similar removal of a nitrogen atom in the 2-pyrimidine series leaving the 2-pyridine analogs only led to modest recovery of the potency in one of the analogs (**5g**, K_i = 730 nM). Substituted 3- or 4-methoxy groups on the phenyl ether were comparable in activity to the unsubstituted phenethyl derivatives (**5p**–**5r**). The 3-fluoro and 4-fluoro substituted compounds were well tolerated resulting in very potent compounds (**5k**, K_i = 10.4 nM; **5l**, K_i = 13.1 nM; **5m**, K_i = 10.8 nM; **5n**, K_i = 10.1 nM). Unexpectedly, the 2-halogen-6-alkoxypyridine compounds were active; unlike the 2-alkoxypyridine analogs (vide supra). In fact, combining the 6-fluoro-3-indole analog (**4ee**) with the 2-chloro-6-alkoxypyridine led to one of the most potent compounds from this series (**5y**, K_i = 3.3 nM). Lastly, two compounds in which the sulfide linker replaced the alkoxy linker were synthesized; this proved to be a fruitful change as well (**5aa**, K_i = 9.4 nM; **5bb**, K_i = 7.4 nM).

Having identified a number of active D_4R antagonists, we next wanted to profile these compounds against the other dopamine receptors (D_1, D_{2L}, D_{2S}, D_3, and D_5) (Table 3). Generally speaking, the compounds are selective against the D_1-like family of receptors (D_1 and D_5), both the phenoxy (**4**) and substituted phenoxy or heteroarylalkoxy compounds (**5**) are selective against the D_1-like family of receptors. The compounds are less selective for the D_2-like family, specifically the D_{2S} and D_{2L} receptors. That being said, a number of compounds prove completely selective against all of the dopamine receptors (Table 3), despite high sequence homology. Notably, the 6-fluoro-3-indole compound (**4ee**) showed activity against both D_{2L} and D_{2S} (78% and 76%, respectively). However, the comparator 2-halogen-6-alkoxypyridine compounds (**5u** and **5y**) were fully selective against all of the dopamine receptors tested. Gratifyingly, **5y** is one of the most potent analogs that was made and tested. In addition, the sulfide analogs were also selective (**5aa** and **5bb**).

Having identified a number of potent and selective compounds, we further profiled selected compounds in a battery of Tier 1 in vitro DMPK assays (Table 4). The intrinsic clearance (CL_{INT}) was assessed in liver microsomes (rat and human), and many of the compounds proved to be unstable to oxidative metabolism and were predicted to display high clearance in both species.[15] However, a few compounds were shown to have moderate predicted clearance, such as **4t** (imidazo[1,2-*a*]pyridine) and **4g** (3-fluoro-4-chlorophenyl), which presumably can block oxidation of the phenyl group. Utilizing an equilibrium dialysis approach, the protein binding of the compounds was evaluated in both human and rat plasma. The fraction unbound (F_u) ranged from low to moderate, and these values loosely correlated with the calculated log*P* of the compounds. Although it is understood that fraction unbound is a difficult parameter to SAR around, lowering *c*Log*P* within a series can tend to produce better values. As such, **4t**, **4l**, and **4y** had the highest fraction unbound and the lowest *c*Log*P* values. Lastly, we assessed the ability of these compounds to cross the blood–brain barrier in a rodent IV cassette experiment to determine brain-to-plasma ratios (K_p).[16,17] A selection of compounds is shown in Table 3, and, although the compounds show high clearance in rat, the compounds are able to cross the BBB with K_p values >2.

In order to better understand the nature of the instability in liver microsomes in both human and rat, we analyzed **5y** in a metabolic soft-spot experiment (Q^2 Solutions, www.q2labsolutions.com). **5y** was highly metabolized in both rat and human liver

Table 1
Structure and D_4 activity of the *N*-linked analogs

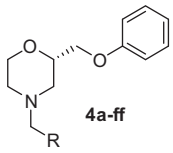

4a-ff

Compound	R	*c*Log*P*[a]	IC_{50} (nM)[b]	K_i (nM)[b]
ML398		5.10	130	36
4a	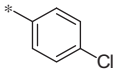	3.73	150	42
4b	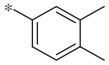	3.68	45	12.3
4c	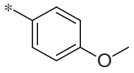	3.08	160	44
4d	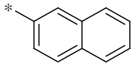	4.40	64	17.8
4e	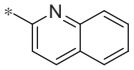	3.15	1110	310
4f	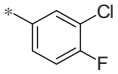	3.84	62	170
4g	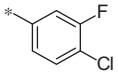	3.84	69	19.1
4h	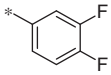	3.54	530	150
4i	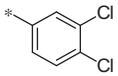	4.35	97	27
4j	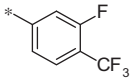	4.21	58	16.2
4k	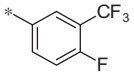	4.21	320	89
4l	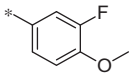	3.18	56	14.3
4m	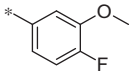	3.18	42	11.6
4n	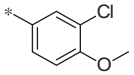	3.70	38	10.4
4o	(*R*)-**4n**	3.70	35%[c]	
4p	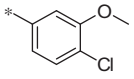	3.70	42	11.6
4q	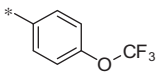	4.48	180	51
4r	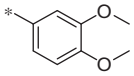	3.04	150	43
4s	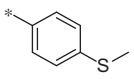	3.75	58	16.1

(*continued on next page*)

Table 1 (*continued*)

Compound	R	*c*Log*P*[a]	IC_{50} (nM)[b]	K_i (nM)[b]
4t	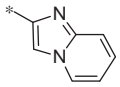	2.89	590	160
4u	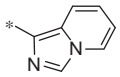	3.51	130	35
4v	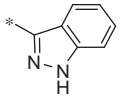	3.73	65	18.1
4w	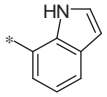	3.77	130	37
4x	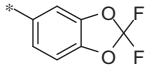	3.83	260	72
4y	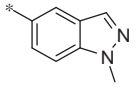	3.20	170	47
4z	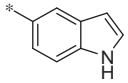	3.77	58	15.9
4aa	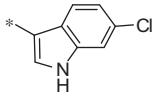	4.39	8.0	2.2
4bb	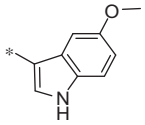	3.73	460	130
4cc	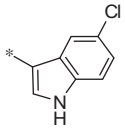	4.39	130	37
4dd	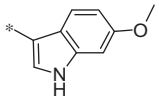	3.73	19.5	5.4
4ee	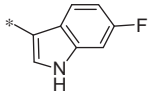	3.87	18.9	5.2
4ff	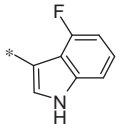	3.87	3830	1060

[a] Calculated using Dotmatics Elemental (www.dotmatics.com/products/elemental).
[b] IC_{50} and K_i values were run in duplicate in a radioligand binding assay using Spiperone at EuroFins (www.EuroFins.com).
[c] % inhibition at 10 μM.

microsomal samples in the presence of NADPH. Compound B was the major metabolite in the rat microsomes (*N*-dealkylation + oxidation), and the major metabolite in human microsomes was Compound A (*N*-dealkylation). The parent compound, **5y**, was observed in the rat and human samples in the absence of NADPH. Thus, further analog work will concentrate on blocking the *N*-dealkylation mechanism of metabolism (see Fig. 2).

In conclusion, we have further elaborated our initial D_4R antagonist, ML398, by changing the ethyl linker to a hydroxymethyl linker on the chiral morpholine scaffold. A number of compounds are very potent (D_4 K_i <20 nM) with excellent selectivity against the other dopamine receptors. Notably, compounds **5y**, **5aa**, and **5bb** were shown to have D_4 K_is <10 nM and be completely selective against the other dopamine receptors (K_is >10 μM, ie., >1000-fold selectivity). Compounds **4ee** and **5y** are intriguing molecules as they contain molecular handles and possess desirable physicochemical properties (*c*Log*P*) for potential radioligand development. Many of the compounds identified were highly cleared in both human and rat liver microsomes, and we have shown that *N*-dealkylation is a major contributor to the

Table 2
Structure and D_4 activity of the *O*- and *N*-linked analogs

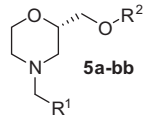

Compd	R^1	R^2	*c*Log *P*[a]	IC_{50} (nM)[b]	K_i (nM)[b]
ML398			5.10	130	36
5a	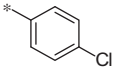		1.83	76%[c]	
5b	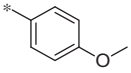		1.17	−4%[c]	
5c	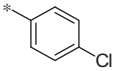		2.33	31%[c]	
5d	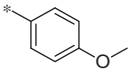		1.67	8%[c]	
5e	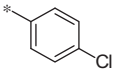		2.42	103	47
5f	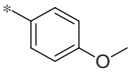		1.77	210	59
5g	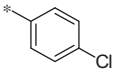		2.83	2,630	730
5h	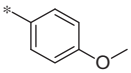		2.17	57%[c]	
5i	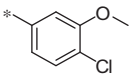		2.79	34%[c]	
5j	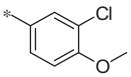		2.79	37%[c]	
5k	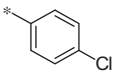	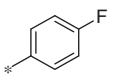	3.84	38	10.4
5l	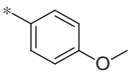		3.18	47	13.1
5m	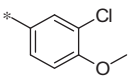	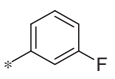	3.80	39	10.8
5n	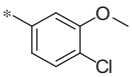		3.80	37	10.1
5o	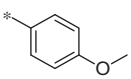		3.18	92	26
5p	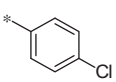	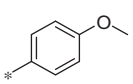	3.70	150	42
5q	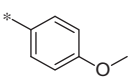		3.04	380	110
5r	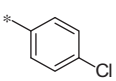	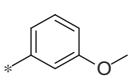	3.70	130	36

(*continued on next page*)

Table 2 (*continued*)

Compd	R^1	R^2	*c*Log*P*[a]	IC_{50} (nM)[b]	K_i (nM)[b]
5s	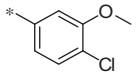	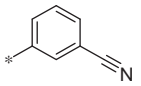	3.41	100	28
5t	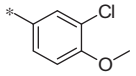		3.41	130	36
5u	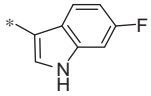	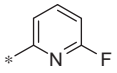	3.47	76	21
5v	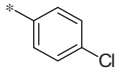		3.33	460	130
5w	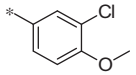		3.30	260	73
5x	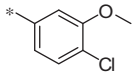		3.30	−3%[c]	
5y	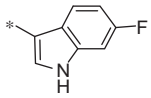	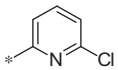	3.99	11.9	3.3
5z	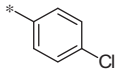		3.85	100	29
5aa	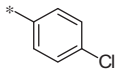	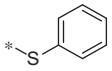	4.41	34	9.4
5bb	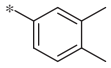		4.35	27	7.4

[a] Calculated using Dotmatics Elemental (www.dotmatics.com/products/elemental).
[b] IC_{50} and K_i values were run in duplicate in a radioligand binding assay using Spiperone at EuroFins (www.EuroFins.com).
[c] % inhibition at 10 μM.

Table 3
Dopamine receptor selectivity of select compounds

Compound	D_4 (nM)	% inhibition at 10 μM[a]				
		D_1 (%)	D_{2L} (%)	D_{2S} (%)	D_3 (%)	D_5 (%)
4b	12.3			<50		
4l	14.3	<50	78	76	<50	
4n	10.4			<50		
4p	11.6	<50	52	60	<50	
4u	35			<50		
4v	18.1			<50		
4z	15.9	<50	64	64	<50	
4aa	2.2	<50	94	93	70	<50
4dd	5.4	<50	87	82	70	<50
4ee	5.2	<50	78	76	<50	
5k	10.4	<50	83	79	51	<50
5l	13.1	<50	88	82	76	<50
5m	10.8			<50		
5n	10.1			<50		
5u	21			<50		
5y	3.3			<50		
5aa	9.4			<50		
5bb	7.4			<50		

[a] % inhibition values were run in duplicate in a radioligand binding assay at EuroFins (www.EuroFins.com).

Table 4
In vitro and in vivo DMPK results of select compounds

Compound	D_4 (nM)	Microsome intrinsic clearance (mL/min/kg)		Plasma unbound fraction (F_u)	
		hCL_{INT}	rCL_{INT}	Human	Rat
4a	12.3	147	4518	0.007	0.007
4g	19.1	65.3	251	0.006	0.012
4i	27	50.5	621	0.002	0.006
4j	16.2	50.5	247	0.002	0.007
4l	14.3	71.9	2128	0.031	0.037
4n	10.4	78.7	1597	0.010	0.019
4p	11.6	79.7	1505	0.010	0.025
4t	160	17.3	154	0.057	0.215
4y	47	60.5	433	0.039	0.074
4z	15.9	135	3137	0.035	0.069
4aa	2.2	46.7	614	0.006	0.010
4dd	5.4	31.6	184	0.037	0.075
4ee	5.2	71.1	1686	0.017	0.047
5m	10.8	93.0	1499	0.006	0.013
5n	10.1	68.9	1774	0.011	0.014
5u	21	101	4010	0.009	0.015
5y	3.3	230	4195	0.015	0.016
5z	29	98.2	5313	0.004	0.008
5aa	9.4	122	3217	0.008	0.005
5bb	7.4	366	6436	0.001	0.004

	Rodent IV cassette (0.25 mg/kg, 0.25 h)		
	Plasma (ng/mL)	Brain (ng/g)	K_p
4a	42.5	197	4.62
4l	14.7	108	7.38
4y	37.3	83.1	2.23
4aa	74.8	246	3.29
5aa	26.1	131	5.03
5bb	23.1	132	5.73

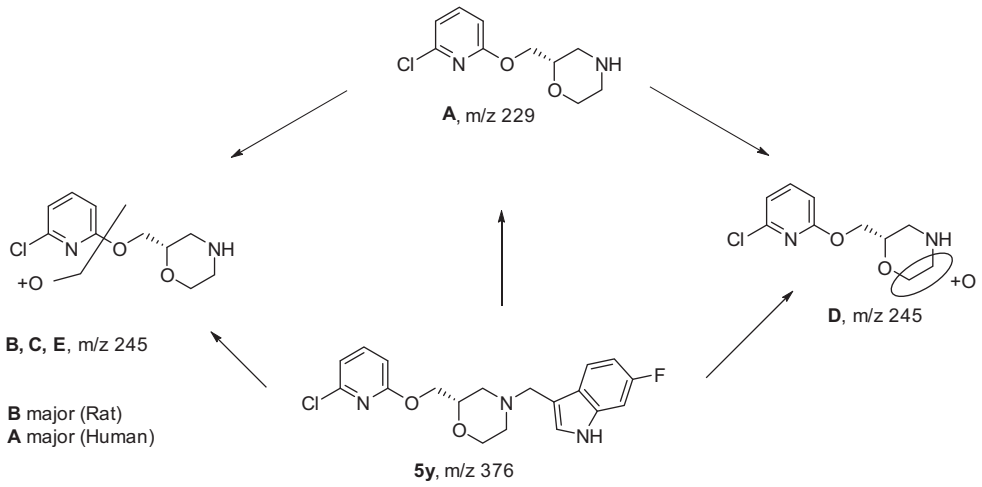

Figure 2. Metabolic soft-spot analysis of **5y** in liver microsomes.

instability. Lastly, compounds from this scaffold class are highly brain penetrant as assessed in a rodent IV cassette experiment to determine brain-to-plasma ratios (K_p values >2). Further optimization and in vivo behavioral efficacy experiments will be disclosed in due course.

Acknowledgments

The authors would like to thank the Michael J. Fox Foundation for Parkinson's Research for research support for CRH (MJFF Grant ID: 10000) and Jarrett Foster, Sichen Chang, and Xiaoyan Zhan for their contributions to the DMPK screening tier.

References and notes

1. Lahti, R. A.; Roberts, R. C.; Cochrane, E. V.; Primus, R. J.; Gallager, D. W.; Conley, R. R.; Tamminga, C. A. *Mol. Psychiatry* **1998**, *3*, 528.
2. Sanyal, S.; Van Tol, H. H. M. *J. Psychiatry Res.* **1997**, *31*, 219.
3. Bristow, L. J.; Kramer, M. S.; Kulagowski, J.; Patel, S.; Ragan, C. I.; Seabrook, G. R. *Trends Pharm. Sci.* **1997**, *18*, 186.
4. Huot, P.; Johnston, T. H.; Koprich, J. B.; Espinosa, M. C.; Reyes, M. G.; Fox, S. H.; Brotchie, J. M. *Behav. Pharmacol.* **2015**, *26*, 101.
5. Huot, P.; Johnston, T. H.; Koprich, J. B.; Aman, A.; Fox, S. H.; Brotchie, J. M. *J. Pharmacol. Exp. Ther.* **2012**, *342*, 576.
6. Di Ciano, P.; Grandy, D. K.; Le Foll, B. *Adv. Pharmacol.* **2014**, *69*, 301.
7. Nutt, D. J.; Lingford-Hughes, A.; Erritzoe, D.; Stokes, P. R. A. *Nat. Rev. Neurosci.* **2015**, *16*, 305.
8. Koob, G. F.; Volkow, N. D. *Neuropsychopharmacology* **2010**, *35*, 217.

9. O'Reilly, M. C.; Lindsley, C. W. *Org. Lett.* **2012**, *14*, 2910.
10. Berry, C. B.; Bubser, M.; Jones, C. K.; Hayes, J. P.; Wepy, J. A.; Locuson, C.; Daniels, J. S.; Lindsley, C. W.; Hopkins, C. R. *ACS Med. Chem. Lett.* **2014**, *5*, 1060.
11. Audouze, K.; Nielsen, E. Ø.; Peters, D. *J. Med. Chem.* **2004**, *47*, 3089.
12. Altman, R. A.; Shafir, A.; Lichtor, P. A.; Buchwald, S. L. *J. Org. Chem.* **2008**, *73*, 284.
13. Mitsunobu, O. *Synthesis* **1981**, 1.
14. *Experimental Procedure for the synthesis of* **5y**: *tert*-Butyl (*S*)-2-(hydroxymethyl)morpholine-4-carboxylate, 1, (110.0 mg; 0.507 mmol) and DMF (2.5 mL) were added to a vial equipped with a stir bar. The mixture was cooled to 0 °C and then NaH (24.3 mg; 0.608 mmol) was added and the mixture was stirred until fully dissolved. Next, 2-chloro-6-fluoropyridine (133.3 mg; 1.013 mmol) was added and then the reaction mixture was warmed to 60 °C. After 90 min, the reaction was cooled to rt and CH_2Cl_2 was added along with 5% LiCl in H_2O. The layers were separated and the organic layer was dried ($MgSO_4$) and collected and concentrated. The crude product was purified via flash column chromatography (5–30% EtOAc/hexanes) to provide the *N*-Boc product. ^{1}H NMR (400 MHz, $CDCl_3$) δ 7.45 (1H, t, J = 8.0 Hz), 6.84 (1H, d, J = 7.5 Hz), 6.64 (1H, d, J = 8.0 Hz), 4.28 (2H, d, J = 4.9 Hz), 3.87 (2H, d, J = 10.6 Hz), 3.72–3.69 (2H, m), 3.51 (1H, dt, J = 11.6, 2.7 Hz), 2.92 (1H, t, J = 22.3 Hz), 2.76 (1H, s), 1.40 (9H, s). The product was treated with 2.0 mL of 4 M HCl/dioxanes and stirred at rt for 30 min. At this time, the mixture was concentrated and the material was converted to the free base via an SCX column. The material was added to a microwave vial along with MP-$CNBH_3$ (88.2 mg; 2.28 mmol/g polymer; 0.201 mmol), acetic acid (23.0 μL; 0.402 mmol) and CH_2Cl_2 (1.0 mL) and then heated in a microwave at 110 °C for 7 min. The reaction mixture was cooled to rt, filtered and washed with CH_2Cl_2 and purified by flash column chromatography (5–30% EtOAc/hexanes) leaving the desired compound (12.0 mg; 0.0320 mmol; 42%). $[\alpha]_D$ +18.84 (c 1.0, CH_3OH); LCMS: R_T = 0.786 min, >98% @ 254 nm, m/z = 376.2 $[M+H]^+$. ^{1}H NMR (400 MHz, $CDCl_3$) δ 8.01 (1H, br s), 7.60 (1H, dd, J = 8.7, 5.5 Hz), 7.42 (1H, t, J = 7.7 Hz), 7.03 (1H, d, J = 1.4 Hz), 6.97 (1H, dd, J = 9.6, 2.0 Hz), 6.84–6.79 (1H, m), 6.63 (1H, d, J = 8.2 Hz), 4.24–4.22 (2H, m), 3.86 (2H, br d, J = 10.9 Hz), 3.68–3.65 (1H, m), 2.80 (1H, d, J = 11.1 Hz), 2.68 (1H, d, J = 11.4 Hz), 2.17 (1H, dt, J = 11.4, 3.2 Hz), 2.00 (1H, t, J = 10.6 Hz); ^{13}C NMR (400 MHz, $CDCl_3$) δ 163.2, 161.3, 158.9, 148.1, 140.6, 136.3, 124.3, 123.8, 120.5, 116.5, 109.5, 108.5, 97.5, 74.1, 67.6, 66.9, 54.8, 54.0, 52.9.

15. Obach, R. S. *Drug Metab. Dispos.* **1999**, *27*, 1350.
16. Smith, N. F.; Raynaud, F. I.; Workman, P. *Mol. Cancer Ther.* **2007**, *6*, 428.
17. Bridges, T. M.; Morrison, R. D.; Byers, F. W.; Luo, S.; Daniels, J. S. *Pharmacol. Res. Perspect.* **2014**, 2.